THE EUROPEAN SOCIETY OF MEDICINE
Medical Research Archives, Volume 13 Issue 4

RESEARCH ARTICLE

Hydralazine Induced Immunologic Response by scRNA-Seq with Olink Proteomics Associated with Survival Time of pancreatic cancer

Baofa Yu, MD [1,2,3,4]; Feng Gao, MD [2]; Peng Jing, MD [2]; Peicheng Zhang, MD [2]; Guoqin Zheng [2]; Shengjun Zhou, MD [2]

[1] Immune Oncology Systems, Inc, San Diego, CA, USA, 92102.
[2] TaiMei Baofa Cancer hospital, Dongping, Shandong, China, 271500.
[3] Jinan Baofa Cancer hospital, Jinan, Shandong, China, 250000.
[4] Beijing Baofa Cancer Hospital, Beijing, 100010.

OPEN ACCESS

PUBLISHED
30 April 2025

CITATION
Yu, B., Gao, F., et al., 2025. Hydralazine Induced Immunologic Response by scRNA-Seq with Olink Proteomics Associated with Survival Time of pancreatic cancer. Medical Research Archives, [online] 13(4).
https://doi.org/10.18103/mra.v13i4.6571

DOI
https://doi.org/10.18103/mra.v13i4.6571

ISSN
2375-1924

ABSTRACT

Background: Pancreatic cancer is a highly lethal cancer with no treatment options when diagnosed at an advanced stage. Hapten combined with chemotherapy drugs have been successfully injected into the tumor for local treatment of pancreatic cancer, but due to the heterogeneity of the tumor, the survival time of patients with similar stages is different.

Methods: SCNA-SEQ and Olink proteomics methods were used to observe the cell and genome changes in the survival group treated with hyrazine combined with HEIC for more than 10 months and less than 6 months. scRNA-Seq shows T cell activity of cDCs and polygene-expressed pDCs.

Results: scRNA-Seq confirmed the initiation of immune response: NaiveT and CD8Teff increased, proliferation increased, NK decreased, and ribosomal protein gene upregulated after treatment. The Neutrophils_4 gene set score of precursor cell neutrophilS_4 was higher. There was high expression of interferon-stimulating gene in neutrophils s_3, and high expression of s_3 characteristic gene set in interferon-associated neutrophils. Due to immune action, proteomic results showed that GZMB, GZMZ, IL18, CASP-8, CD8A, HO-1 and AOA genes were up-regulated by 8%. DCN, MCP-1, CX3cl1, CD40, CD27, IL33, TIE2, Gal-9, PGE, MCP-3, CD28, PD-L1, CD38, CCL3, MCP-2, MMP7, laptgf-β-1 genes were down-regulated by 18%.

Conclusions: Overall, the study showed that patients with similar stages of pancreatic cancer had an enhanced immune response after the same regimen of HEIC treatment, and found that gene expression increased by 8% and decreased by 18% in the longer survival group compared with the shorter survival group due to tumor heterogeneity.

Keyword: Local drug delivery, Hydralazine induces immunity Immune response with local therapy, Hapten enhanc intratumoral therapy, scRNA-Seq, Olink Proteomics.

Introduction

Pancreatic cancer is a highly deadly cancer, and five-year survival rates have changed little over the past few decades. Most patients are diagnosed at an advanced stage due to lack of symptoms or vague symptoms. The choice of treatment depends on the extent of the disease: resectable, borderline resectable, locally advanced, and metastatic. At the same time, the patient's physical condition is also an important consideration of the treatment effect. Few drugs are available to treat pancreatic cancer at late stages.[1, 2]

Immune therapy such as immune checkpoint inhibitors have shown a promising approach.[2] Recent advancement is using hapten enhance intratumoral chemotherapy (HEIC), has been successfully injected into local tumor body to treat advantage pancreatic cancer with resultant prolonged survival of patients and maintaining good quality of life.[3] Hapten modified tumor-associated antigens are released from the tumor injected of cytotoxic drugs with hapten. For example, penicillin as hapten plays an immuno-modulator of tumor epitopes modified by tumor antigens and produces an immune response against the tumor.[3,4] HEIC likes the tumor lysates vaccine to induce immunological response, especially whole cancer cells or cancer cell lysates, it is a very promising approach associated with T cell immunity.[5,6,7] Here we selected hydralazine to replace the penicillin as hapten, hydralazine like penicillin can induce some of adverse reactions effects which caused by immunologic reactions, hydralazine possess the ability to reactivate tumor suppressor gene expression and hydralazine is currently being evaluated, along with histone deacetylase inhibitors either alone or as adjuncts to chemotherapy and radiation.[8, 9,10,11,12] Adverse drug reactions, such as drug-induced lupus, usually involve active intermediates, and the oxidation of hydrazine leads to covalent binding of active intermediates to proteins, which may be related to the induction of lupus by hydrazine. We use haptenization of hydrazine with tumor-associated antigens (TAAs) to convert TAAs into neul TAAs by covalent binding to TAAs proteins.[8, 9,10,11,12]

In the clinical practise, we have found some similar patients with the same treatment, there are still different, some patients survived longer while others survived shorter. What are the causes and factors that lead to the difference in efficacy? Is there tumor heterogeneity, excluding age, tumor stage, and physical condition? There are no reports of heterogeneity analysis for pancreatic cancer.

When physician select an effective treatment, it is not only based on the effect of the treatment for local tumor, also depends on whether the treatment could bring a potential immune response to control tumor at distance of primary tumor. There is no single drug, even combination drugs to have both roles of control local tumor and distance tumor like the HEIC. New tech of scRNA-Seq was used to confirm initiation of immunity following HEIC intratumoral injection and genomic and functional heterogeneity of complex biological systems were analyzed by Olink proteomics technology, while evaluating tens of thousands of cells and revealing regulation, communication, and interactions between cells and cytokines of production following HEIC.[5,6,7]

This study provides a details at single cell and molecular level with regard to the cell composition changes of ProliferatingT, NK, NaiveT, CD8Teff for activation of immune response, followed the changes of cytokines before and after HEIC to primary pancreatic cancer and compared with each group survival time longer and short.

Materials and Methods

CLINICAL SPECIMENS

The informed consent form was signed by the patients and their family members, and this experiment was approved by the Ethics Committee Board of Shandong Baofa Cancer Institute (TMBF 0010, 2015). All method for experiments were performed in accordance with relevant guidelines and regulations.

Two groups of 28 pancreatic cancer patients were retrospectively selected, one group of survived over 10 months (A) and one group of survived less than 6 months (B) with pathology diagnosis for adenocarcinoma of the pancreas and lymph nodes metastasis (II-IV) (Table 1-2), treated with hapten-enhanced intra-tumoral chemoimmunotherapy (HEIC), which included 1.00 mg/ml Adriamycin (Adr), 0.80 mg/ml of cytarabine (Ara-C), 20.0 mg/ml of H_2O_2 and 144mg/ml of hydralazine （Hyd） as hapten.[3,4,8] The patient's blood samples were collected on the day before and one weeks later following the first treatment. Some of the blood samples (3ml) were collected immediately stored in GEXSCOPETM Tissue Preservation Solution (Singleron, Cologne, Germany). All patient's blood samples were continuously collected and stored in EDTA, plasma was obtained by centrifugation (3,000rpm for 15min at 4°C) and stored at −80°C for Olink Proteomics.[13,14] All patients were followed up for analysis of survival time, then each group's blood samples were arranged as A group and B group were carried out for Olink proteomics.

SEQUENCING DATA PROCESSING AND QUALITY CONTROL

The fresh samples of blood were stored in SCelLiVeR tissue preservation solution in GEXSCOPER (Singleron) till molecular testing.[5] Original gene expression matrix data were generated using the CeleScopeR (https://github.com/singleron-RD/CeleScope) software. CeleScopeR is a single-cell data processing software developed by Singleron.quality control and filter the data was carried.[6] Reads were compared with the reference genome GRCh38 with ensemble version 93. Gene annotation was used STAR (version 2.6.1b).[6,7] Differentially expressed genes (DEGs) analysis (Scanpy) Identify differentially expressed genes (DEGs) was studied by using the scanpy.tl.rank_genes_groups function based on the Wilcoxon rank sum test with default parameters and selected the genes expressed in more than 10% of the cells with an average log (Fold Change) value greater than one as DEGs.[7]

Cell type annotation Cell type identity in each cluster was determined by the expression of canonical markers found in the DEGs using the SynEcSys database (Singleron Biotechnologies).[7]

Subtyping of major cell types, CNV detection was based on scRNA-seq and pathway enrichment analysis to

investigate the potential functions of DEGs between clusters, the Gene Ontology (GO) and Kyoto Encyclopedia of Genes and Genomes (KEGG) analysis with the "ClusterProfiler" R package 3.16.1.[6] Gene set variation analysis GSVA) pathway enrichment analysis.[7]

UCELL GENE SET SCORING

Gene set scoring was performed using the R package UCell v 1.1.0. [7] UCell scores based on the Mann-Whitney U statistic by ranking query genes in the order of their expression levels in individual cells.

TRAJECTORY ANALYSIS

We used the R package monocle (version 2.18.0)[10] to carry out single-cell trajectory analysis, and the dimensionality reduction method was DDRTree.[7] Transcription factor regulatory network analysis (pySCENIC)

The transcription factor network was constructed by pySCENIC (v0.11.0) and the scRNA expression matrix and transcription factors in AnimalTFDB. AUCell.[24,7]

CELL-CELL INTERACTION ANALYSIS

Cell-cell interactions (CCI) between different cell types were predicted based on known ligand-receptor pairs by Cellphone DB v2.1.0.[15] Predicted interaction pairs with p-value < 0.05 and average log expression > 0.1 were considered significant. Differentially activated ligand-receptor pairs between groups were visualized by dot plot in ggplot2.[5,6,7]

PROTEOMICS ASSAY

Plasma cytokines markers were assessed using the commercially available Olink® Target 96 Inflammation panels from Olink (Uppsala, Sweden). In brief, the target protein binds to the double oligonucleotide-labeled antibody probe with high specificity, and then the microfluidic real-time PCR amplification of the oligonucleotide sequence is used to quantitatively detect the resulting DNA sequence. Using internal and external controls, the resulting 1 https: //olink.com Bao et al.[13,14]

DEP ANALYSIS

The R package "Olink®Analyze" was used to identify the sets of DEPs between the two groups. Proteins with a p-value of <0.05 were considered to be differentially expressed. The visualization of DEPs including volcano plots and heatmaps was performed by using the standard R package "ggplot2." The diagnostic performance of DEPs was assessed by receiver operating characteristic (ROC) curves. AUC was recorded as an index of diagnostic accuracy and compared among the proteins. According to logistic regression, two or more indicators were combined, and AUC value of the combined diagnosis is shown in the figure legend at the lower right corner so that the combined diagnostic effect can be viewed. A higher AUC value reflected the greater performance of the classifier. The AUC value of 1.0 represented a perfect assignment, whereas an AUC of 0.5 represented an unreliable test (gray line).

GO ENRICHMENT ANALYSIS AND PATHWAY ENRICHMENT ANALYSIS

All GO terms that were significantly enriched in DEPs compared to the genome background are provided by GO enrichment analysis. The "ggplot2" R tool was used to visualize the findings of GO and KEGG enrichment analysis, and the top 20 GO terms and KEGG pathways were shown as a bubble chart.

CORRELATION ANALYSIS

Pearson's correlation analysis was used to determine the correlation between the expression levels of two DEPs, and the scatterplots illustrated the strongest correlation. Pearson correlation tests were also employed to analyze the correlation between the DEPs and clinical features of patients. The significance of correlation coefficients was calculated using the p-value calculator for correlation coefficients.[13]

STATISTICAL ANALYSIS

All statistical analyses were performed using the R software "Olink®Analyze" (V.2.0.0). A value of p of less than 0.05 was considered statistically significantly.[13,14]

Result

CLINICAL AND POST-TREATMENT RADIOLOGICAL CHARACTERISTICS: All studies showed the patient's conditions and survival time was significantly difference between patient's life longer over 10 months and less 6 months (Table 1 and 2).

scRNA-Seq landscape

A total of 5 cell types were obtained, namely Bcells, TandNK, Neutrophils, MPs and Platelets. The proportion of neutrophils increased significantly, the proportion of lymphocytes (B and T cells) and myeloid cells (MPs) decreased after treatment (Fig. 1 A-D). The proportion of NaiveT and CD8Teff increased, Proliferating and NK decreased, the inflammatory and virus-related gene scores of NK and CD8TeffT cells increased and NaiveT decreased, ribosomal protein genes were up-regulated after treatment (Fig. 1 E-F).

Fig. 1

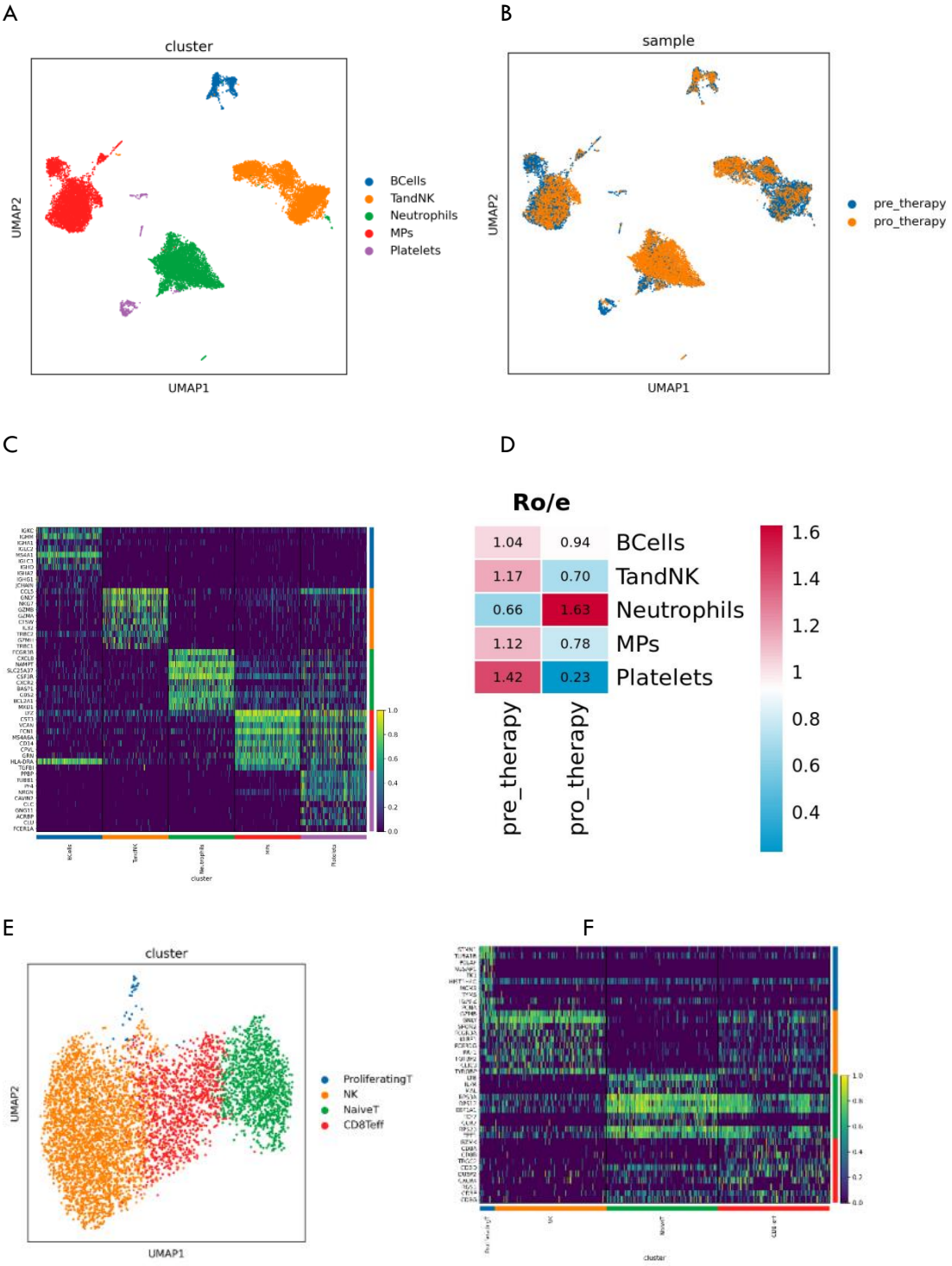

A: UMAP cell group map was formed by dimensionality reduction clustering. Different colors represent different cell types;
B: The distribution of various cell types before and after treatment, with blue representing before treatment and yellow representing after treatment;
C: Heat map showing the Top10 differential genes of each cell type;
D: Ro/e chart of the proportion of various cell types before and after treatment.
E: TandNK was subdivided and UMAP cell cluster map was formed by dimensionality reduction clustering; Different colors represent different cell types;
F: Heat map display of Top10 differential genes of each cell type.

MPs were subdivided into ClassicalMono, NonClassicalMono, cDCs, and pDCs after treatment, the proportion of classical monocytes increased and the proportion of non-classical monocytes decreased. ClassicalMono can be further subdivided into ClassicalMono_1 and ClassicalMono_2. before treatment, ClassicalMono_1 was the main monocyte population, and after treatment ClassicalMono_2 became the main classical monocyte population (Fig.2 A-F).

Neutrophils_1, Neutrophils_2, Neutrophils_3 and Neutrophils_4 were further subdivided, the proportion of Neutrophils_2 increased and the proportion of Neutrophils_3 decreased significantly after treatment. The score of Neutrophils_1 was higher than that of pro inflammatory neutrophil characteristic gene set. The score of Neutrophils_2 in promoting angiogenesis of neutrophils was higher. Differential gene analysis of

neutrophils before and after treatment showed that neutrophils highly expressed pro-metastasis factor PLAU.

Fig. 2

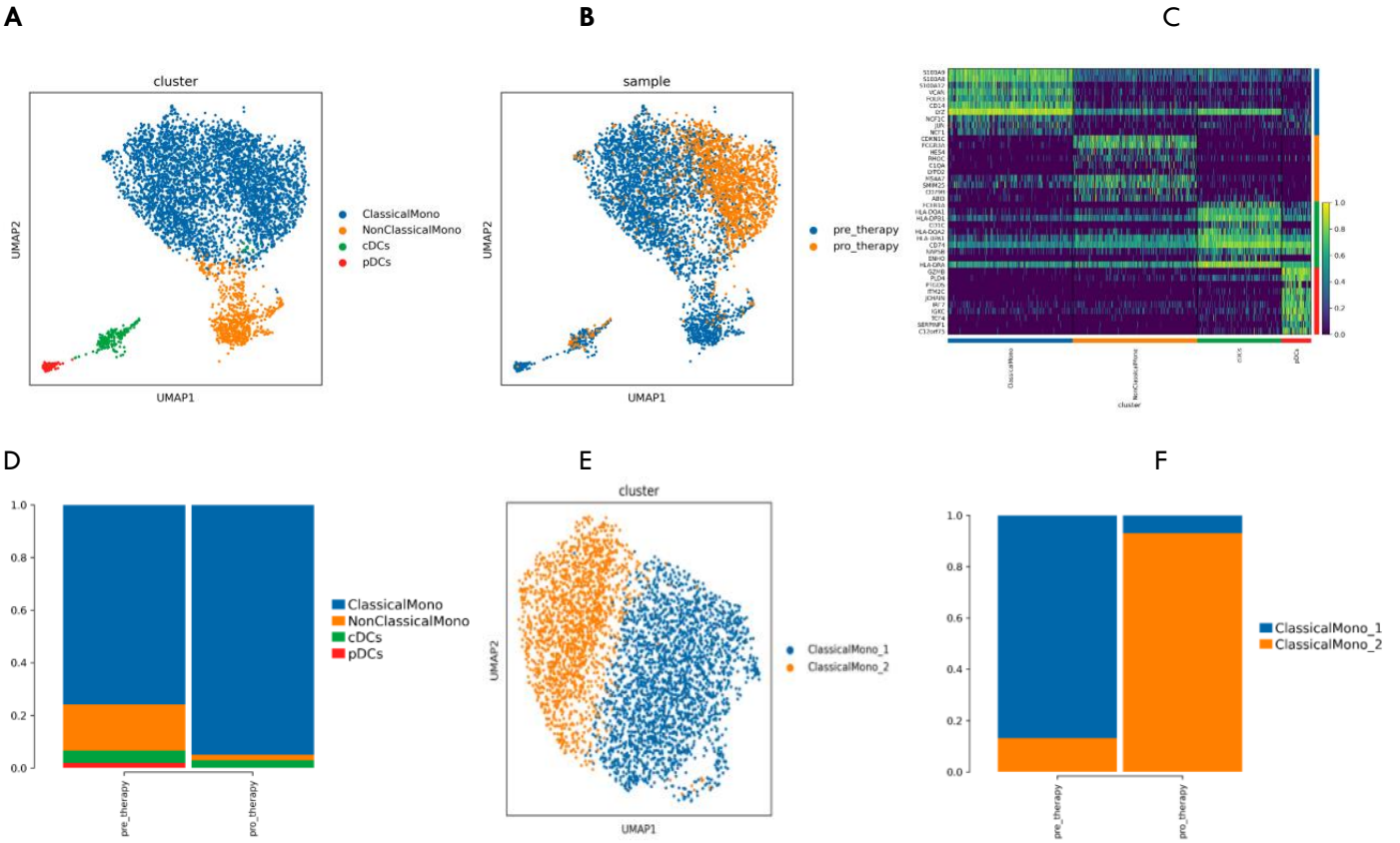

Fig. 2

A: MPs were subdivided and UMAP cell cluster map was formed by dimensionality reduction clustering. Different colors represent different cell types;

B: Distribution of various cell types before and after treatment, with blue representing before treatment and yellow representing after treatment;

C: Heat map display of Top10 differential genes of each cell type;

D: Histogram of the proportion of various cell types before and after treatment;

E: Subdivide ClassicalMono and form UMAP cell group map by dimensionality reduction clustering; Different colors represent different cell subtypes;

F: Histogram of the proportion of the two cell types before and after treatment;

Olink Proteomics Landscape

Analysis of protein expression: ggpubr package was used to draw box plots for each protein expression in the long survival group and the short survival group respectively, and the significance was marked based on subsequent statistical analysis. Through the results, the degree and significance of difference in NPX expression value of the same protein under different experimental conditions could be clearly found (Fig.3 A). The box diagram of the expression levels of 92 proteins, and the high-definition picture can be looked in attached (/backup/QPE/Olink_box_sig_anova_backup.pdf).

Differential protein analysis between two groups: The proportion of differential protein and non-differential protein in Olink project was analyzed (Fig.3-B). Cluster heat map of different proteins between the groups. Based on the NPX value of the protein significantly up-regulated or down-regulated obtained by the above statistical analysis, the cluster heat map is drawn after z-score processing, high-definition images (Fig. 3C), (" /backup/Diff_pro/Olink_volcano_*_sig_gene_heatmap .pdf). Based on the above statistical analysis results, ggplot2 was used to draw a volcano map, which could well show the degree of up-regulated and down-regulated differential protein distribution. The diagram shows a volcanic map of the difference analysis between the two sets of data (Fig.3 D). Detailed results can be found in the annex (" /result/04.Diff_pro/Olink_*_volcano. *).

Differential protein functional enrichment analysis: The general functional databases has provided annotations in this study mainly include GO, KEGG, COG, etc. Functional annotation of the identified proteins was conducted using these databases to understand the functional properties of different proteins, and biological functional enrichment analysis was performed on the differential proteins through GO (Gene Ontology Analysis) and KEGG (KEGG Pathway Analysis). Enrichment fractions of differential proteins in each biological pathway and process were obtained, and enrichment bar charts and bubble charts were drawn (Fig.3 E).

Fig. 3

Fig. 3-A

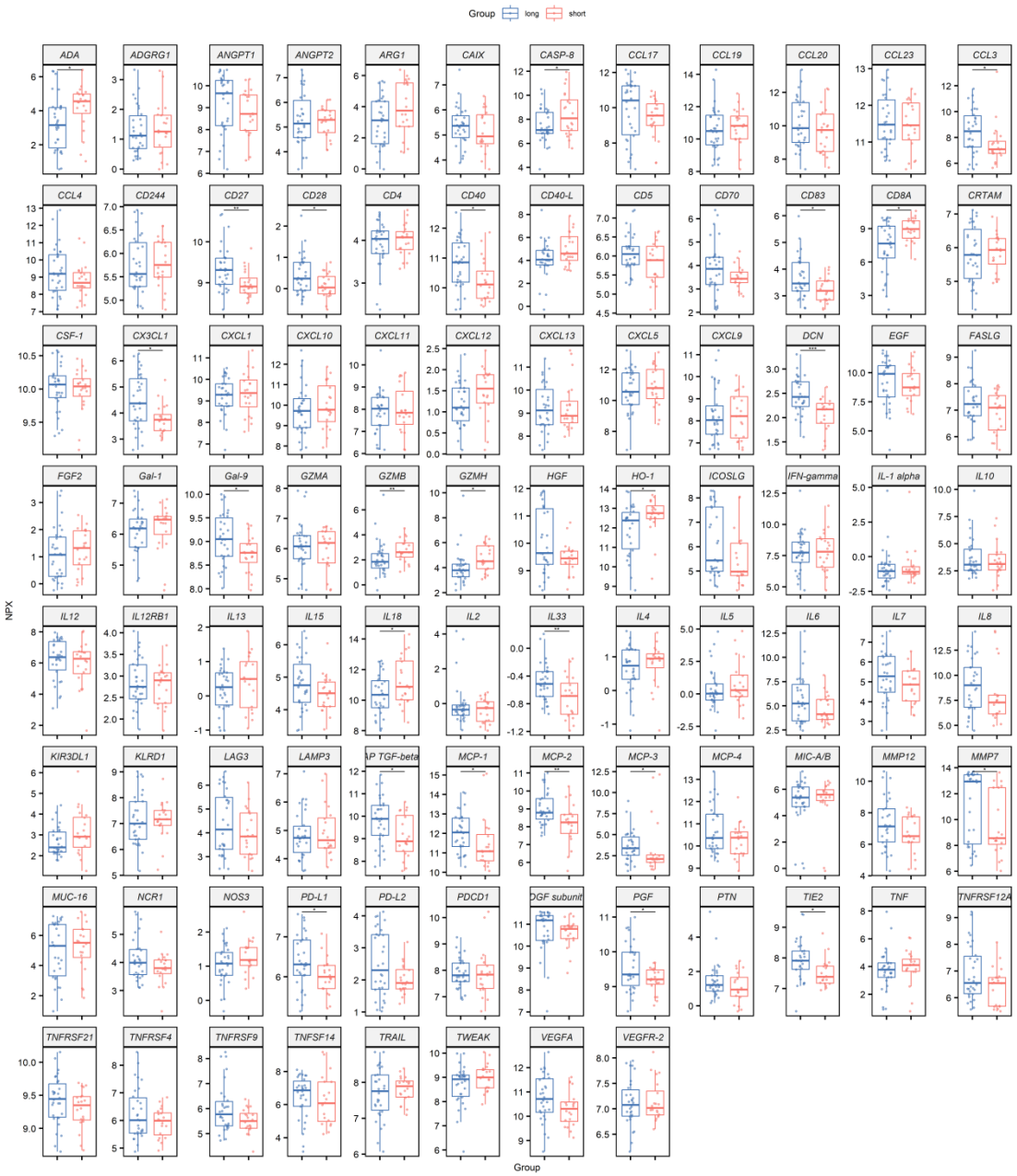

Fig. 3-B

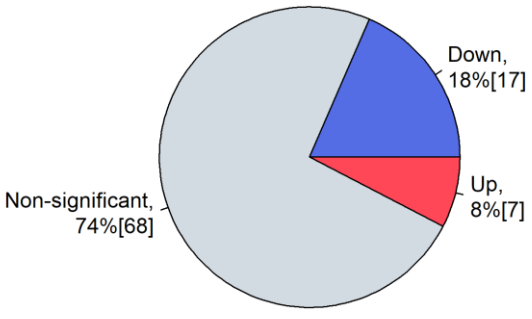

Fig. 3-C

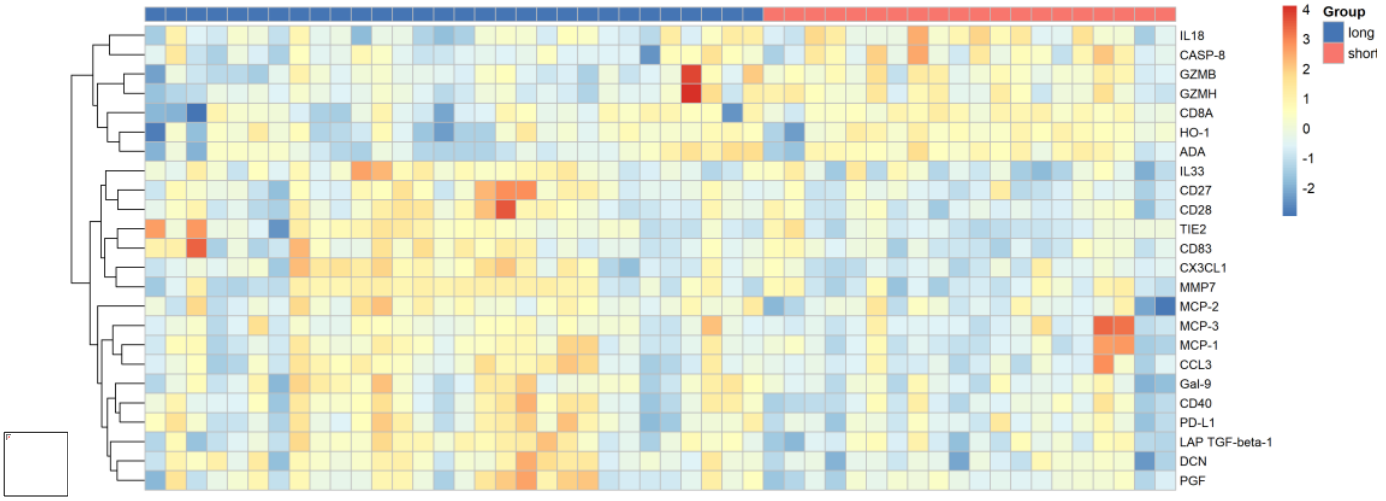
IL18
CASP-8
GZMB
GZMH
CD8A
HO-1
ADA
IL33
CD27
CD28
TIE2
CD83
CX3CL1
MMP7
MCP-2
MCP-3
MCP-1
CCL3
Gal-9
CD40
PD-L1
LAP TGF-beta-1
DCN
PGF
4
3
2
1
0
-1
-2
Group
long
short

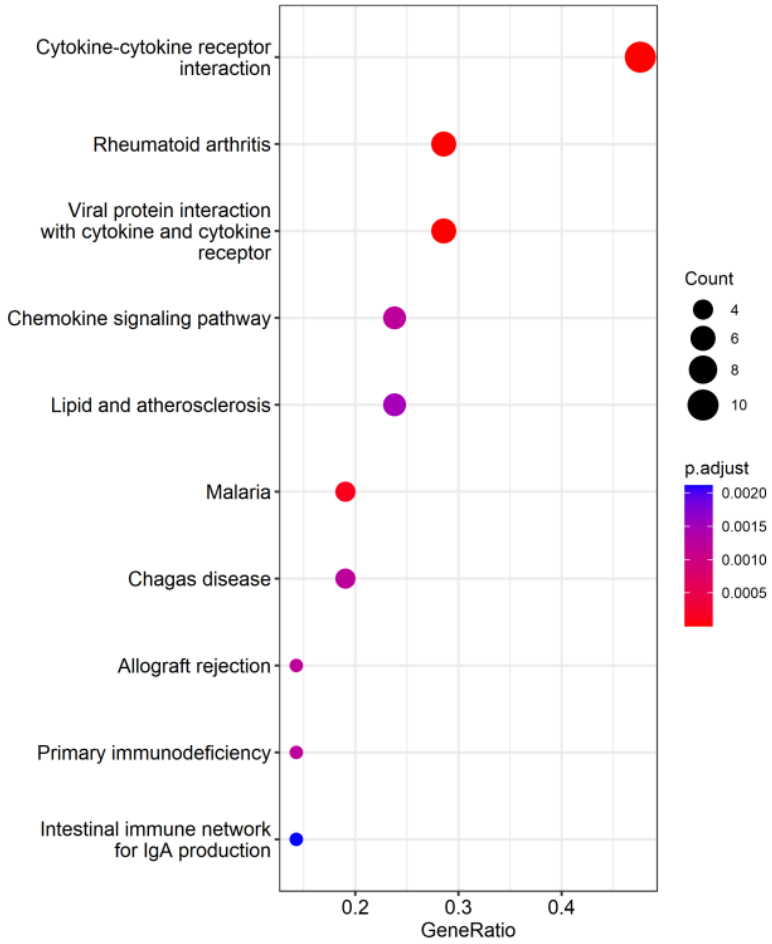
Cytokine-cytokine receptor interaction
Rheumatoid arthritis
Viral protein interaction with cytokine and cytokine receptor
Chemokine signaling pathway
Lipid and atherosclerosis
Malaria
Chagas disease
Allograft rejection
Primary immunodeficiency
Intestinal immune network for IgA production
0.2
0.3
0.4
GeneRatio
Count
4
6
8
10
p.adjust
0.0020
0.0015
0.0010
0.0005

Fig. 3-D

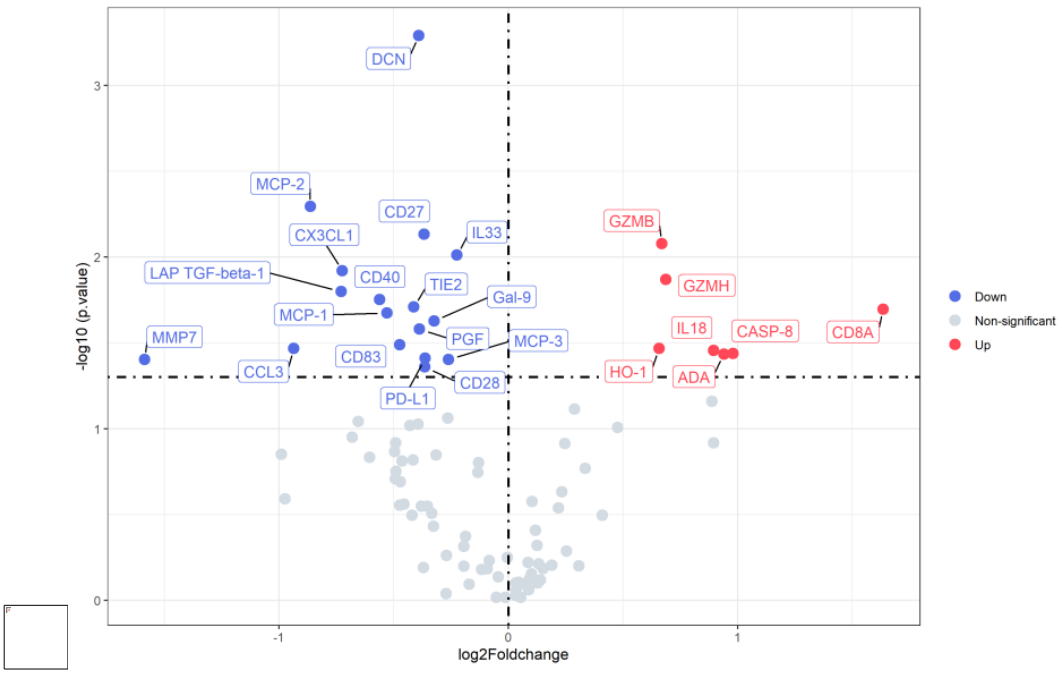

Fig. 3-E (E1,E2)

E1

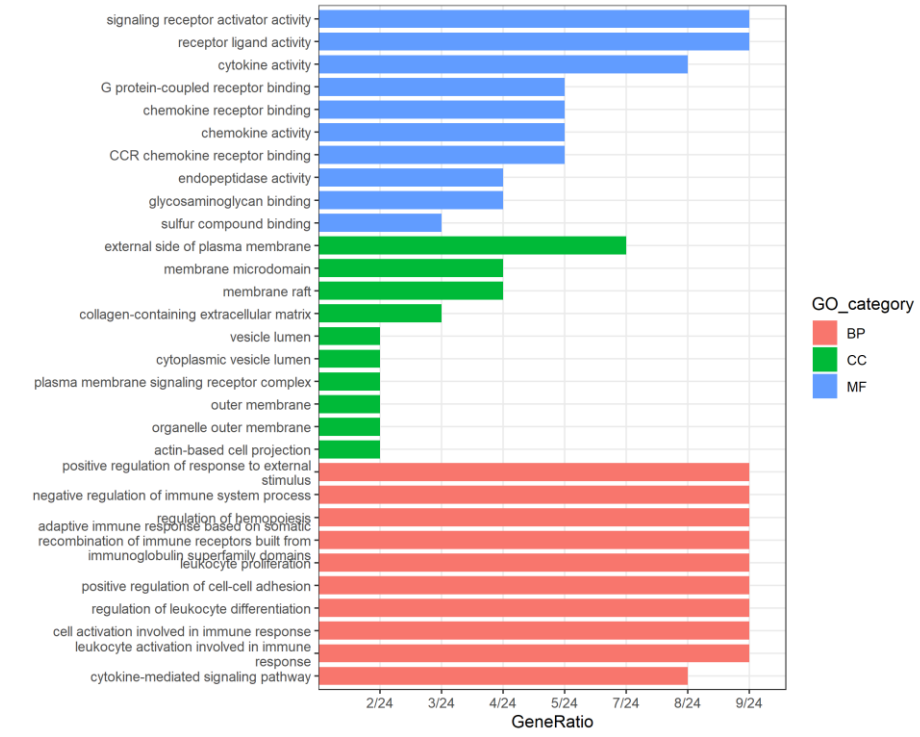

E2

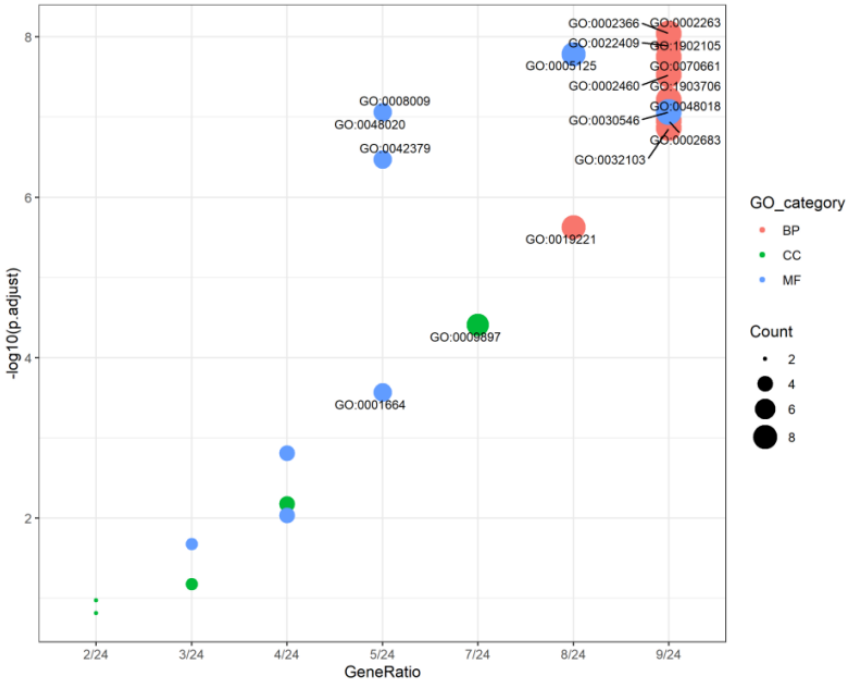

Fig.3-F (F1, F2)

F1

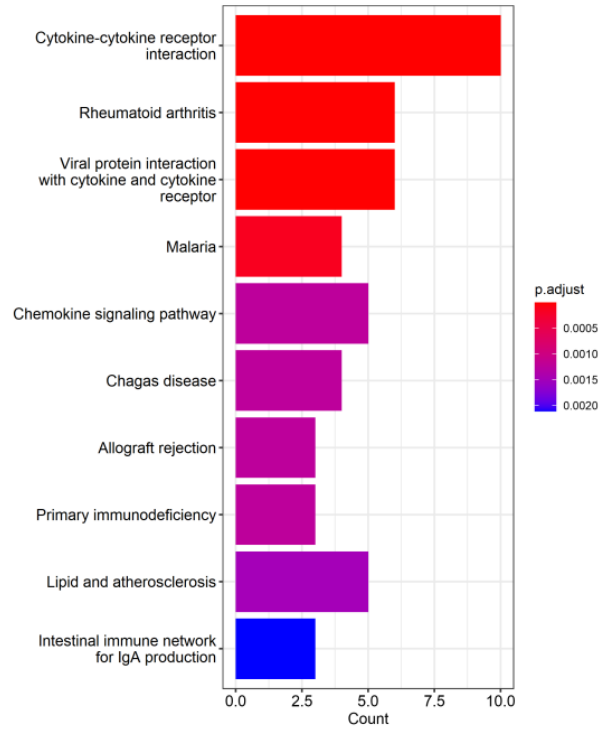

F2

A: The box diagram for the expression levels of 92 proteins and the high-definition picture is attached (/backup/QPE/Olink_box_sig_anova_backup.pdf).

B: Red represents significantly up-regulated differential protein proportion; Blue is significantly down-regulated differential protein proportion; Gray is the proportion of non-significant difference protein.

C :The horizontal coordinate of Panel differential protein clustering heat map is the sample name, the vertical coordinate is Panel differential protein, and the legend annotation Group is different groups.

D: All differential proteins (genes) were labeled according to significance threshold (p-value < 0.05) segmentation. The horizontal coordinate is the difference between the groups. Since NPX is the value after log2 processing, fold change is log2foldchange; The ordinate uses -log10 (p-value) to represent the negative logarithm of the p-value of the significance of the T-test. The horizontal dotted line is p-value = 0.05, and the vertical dotted line is foldchange=0. The red dots represent significantly up-regulated differential genes, the blue dots represent significantly down-regulated differential genes, and the gray dots represent non-significant differential genes.

E: E1: Significance difference GO enrichment histogram

E2: Significant difference GO enrichment drum diagram

F: F1: Differential kegg enrichment histogram;

F2: Differential kegg enrichment drum diagram

KEGG PATHWAY ANALYSIS: The annotation results of the pathway of differentially expressed proteins are shown in the following figure. The whole pathway is composed of complex biochemical reactions catalyzed by multiple enzymes. The enzymes related to differentially expressed genes in this pathway map are marked with different colors. For the enzyme number down-regulated, the specific sequence information and biological function information of the enzyme can be queried in the KEGG database online website (Fig. 3F).

Discussion

Pancreatic cancer is one highly lethal cancer, even cancer is still localized, the most of patients is already advanced stages at the time of diagnosis.[1,2] Hapten plus cytotoxic drugs have been successfully treated pancreatic cancer with prolonged survival and good quality of life. The penicillin was used as hapten to modified by tumor antigens and produces an immune response against the tumor.[3,4]We found that a difference is the survival time for similar patients in the same stage.

scRNA-seq analysis has confirmed the changes of immune cells from blood followed patient treatment of HEIC, it was found that the proportion of lymphocytes (B and T cells) and myeloid cells (MPs) decreased significantly. The proportion of NaiveT and CD8Teff increased while proliferating and NK decreased, the ribosomal protein genes were up-regulated (Fig. 1A-F). Few studies on ribosomal genes have showed that high expression of ribosomal protein-related genes indicated that B cells were in a relatively late stage of germinal reaction.[15] There was also a study on breast cancer that showed that ribosomal proteins promote cancer cell migration and spread.[16]

In this study, MPs is subdivided into ClassicalMono, NonClassicalMono, cDCs, and pDCs after treatment, the proportion of classical monocytes increased while the proportion of non-classical monocytes decreased (Fig. 2A-F). The differential gene enrichment analysis of classical monocytes of the two subgroups showed that ClassicMono_1 was enriched in the signaling pathways related to immune cell activation and immune response, while ClassicMono_2 was enriched in the MHC protein complex and other pathways in addition to the high enrichment of ribosome related genes from the point of view of the score.

In this study, it has indicated the proportion of Neutrophils_2 increased and the proportion of Neutrophils_3 decreased significantly after treatment. According to four neutrophils subgroup of the top 10 ratings found genes and neutrophil function set, Neutrophils_3 highly expressed interferon-stimulating genes including IFIT1, IFIT2, IFIT3, ISG15 and RSAD2,[16] Differential gene analysis of neutrophils before and after treatment showed that neutrophils highly expressed pro-metastasis factor PLAU,[17] and pro-tumor factor IL1RN.[18]

It was also found that Holistic heat maps of pre and post treatment cell communication demonstrate enhanced interactions between T cells, neutrophils, and monocytes, CD28_CD86 enhanced the interaction between lymphocytes and classical monocytes after treatment. Studies has showed that CTLA-4 competed with CD28 to bind CD80 and CD86, and CD28 could activate T cell activation.[19] At the same time, the interaction of LGALS9_HAVCR2 also increased after treatment, suggesting the potential immunosuppressive capacity of this monocyte subpopulation.[20,21] After treatment, major lymphocytes (CD8Teff and NK) interact with major classical monocytes (ClassicMono_2) in the form of CCL5_CCR1, and studies have shown that CCL5 is associated with M2 polarization of macrophages. Immune complexes with protein as antigen scRNA-Seq has confirmed the activity of initiates an immune response following the treatment of HEIC with hydralazine which indicated hydrazine can bind to the TAAs to form Immune complexes with protein and hydrazine as neoantigen.[8,9,10]

As result of immune response followed HEIC, the proteomics has confirmed that a up 8% cytokines while 18% down of cytokines in long survival group compared with short survival group (Fig. 3 A to F). The higher of cytokines were GZMB, GZMZ, IL18, CASP-8, CD8A, HO-1, AOA; the down of cytokines were DCN, MCP-1, CX3cl1, CD40, CD27, IL33, TIE2, Gal-9, PGE, MCP-3, CD28, PD-L1, CD38, CCL3, MCP-2, MMP7, LAPTGF-bete-1, each of them has own function, all work together has played a “Yin and Yang" role in bi-directional comply interaction for control overall cancer growth.[25-31] The treatment of HEIC induced the immune response by hydralazine modified immune complexes with protein as neo antigen for the whole pathway of differential expressed protein pathway is composed of complex biochemical reactions catalyzed by multiple enzymes. For up-regulated enzyme numbers, specific sequence information and biological function information of the enzyme are available in the KEGG database (Fig.3 E), these enzymes have played a role for regulation of those cytokines of genes in order to control carcinoma cells.

After treatment of HEIC, cDCs, and pDCs up-regulated MHC II signaling pathway activity, NaiveT and CD8Teff increased. It resulted in the up expression of these cytokines of genes and control down expression of those cytokines of genes, further resulted in long survival group compared with short survival group. It was found that the group of longer survival patients has up 8% expression of genes and down 18% expression of the genes, the difference may be during to the heterogeneity of immune cells individual and tumor environment between the two groups.[32,33]

This significant difference may be related to the heterogeneity of immune cell individuals and pancreatic cancer has been reported to be a highly heterogeneous disease at the single-cell level.[34] The high expression of 8% genes of longer survival patients and the low expression of 18% genes in long surviving patients indicate the combined effect of these gene products, and the cancer growth height is reduced, and finally achieves the therapeutic effect. At the perspective of immune drugs, it is impossible to have so many factors of immune drugs to treat patients at the same time, however it is possible to induce a multi-factor immunotherapy locally intratumoral with multi hapten plus drugs or new mRNA

vaccine of GZMB, GZMZ, IL18, CASP-8, CD8A, HO-1, AOA.

Finally, further analysis with more patients treated by different or multi hapten is needed to overcome a comprehensive heterogeneity of immune cells individual and tumor environment.

Authors statement:

Baofa, Yu, MD: conceived the concept and provided overall supervision of all
Feng Gao, MD: Helped the clinical sample collection
Peng Jing, MD: He helped the clinical data collection.
Peicheng Zhang, MD: He collected clinical samples
Guoqin Zheng, MS: She conducted and communicated with single cell company and data analysis.
Shengjun Zhou, MD: Collected the clinical samples

Conflict of Interest Statement:

All of authors does not have any conflict interest for the research.

Ethical Statement:

All procedures and protocols for the study have been reviewed and approved by the Ethical Committee of the Beijing Baofa Cancer Hospital (TMBF 0010, 2015). All informed consent forms from patients have been signed prior to the start of the study. Ethical Approval: approved by the Ethical Committee of the Beijing Baofa Cancer Hospital (TMBF 0010, 2015). Funding Sources:

Data Availability Statement

The data that support the findings of this study are available from [third party name] but restrictions apply to the availability of these data, which were used under license for the current study, and so are not publicly available. Data are however available from the authors upon reasonable request and with permission of [third party name].

Funding: There is not outside funding for this research.

Financial support

This study was sponsored in part by Tai Mei Baofa Cancer Hospital, Dongping, Shandong Province, China 271500.

Author contributions

Yu B designed the concept of the experiments. The first draft was written by Yu B. All authors were involved in the subsequent versions of manuscript, the final version was written by Yu B. All authors read and approve the final manuscript.

Competing Interests

The authors declare no competing interests.

Availability of Data and Materials

The data that support the findings of this study can be requested from Professor Baofa Yu, MD. He can be reached via e-mail at: baofa@oncologysystems.com, bfyuchina@126.com; however, the materials are not available for the samples used for these studies were from patients' biopsies not from immortal cell lines.

Financial support

This study was sponsored in part by Tai Mei Baofa Cancer Hospital, Dongping, Shandong Province, China 271500.

References

1. Mizrahi JD., Surana R., Valle JV., et al. Pancreatic cancer. Lancet. 2020 Jun 27;395(10242):2008-2020. doi: 10.1016/S0140-6736(20)30974-0.
2. Neoptolemos JP., JKleeff J., Patrick Michl P. et al. Therapeutic developments in pancreatic cancer: current and future perspectives. Nat Rev Gastroenterol Hepatol. 2018 Jun;15(6):333-348. doi: 10.1038/s41575-018-0005-x.
3. Yu B.F., Han Y., Fu Q., et al. Awaken Immune Cells by Hapten Enhanced Intratumoral Chemotherapy with Penicillin Prolong Pancreatic Cancer Survival. Journal of Cancer.2023; 14(8): 1282-1292. doi: 10.7150/jca.82985.
4. Yu B.F., Fu. Q., Han Y., Zhang J., Chen D. (2022). An Acute Inflammation with Special Expression of CD11 & CD4 Produces Abscopal Effect by Intratumoral Injection Chemotherapy Drug with Hapten in Animal Model. J Immunological Sci 6, 1-9.
5. Kechin, A., Boyarskikh, U., Kel, A., et al. cutPrimers: A New Tool for Accurate Cutting of Primers from Reads of Targeted Next Generation Sequencing. J Comput Biol. 2017 Nov; 24(11):1138-1143. doi: 10.1089/cmb.2017.0096. Epub 2017 Jul 17.
6. Yu, B., Gao, F., Jing, P., et al. Cancer Immunotherapy Preparation and Immune Cells Activation through Hapten-Enhanced Chemotherapy in Primary Lung Cancer. J Basic Clin Pharma. 2023, 14(S1):10-16.
7. Dobin, A., Davis, C.A., Schlesinger, F., et al. STAR: ultrafast universal RNA-seq aligner. Bioinformatics. 2013 Jan 1; 29(1):15-21. doi: 10.1093/bioinformatics/bts635. Epub 2012 Oct 25.
8. Arce C., Segura-Pacheco B., Enrique Perez-Cardenas E., et al. Hydralazine target: from blood vessels to the epigenome. J Transl Med. 2006 Feb 28:4:10. doi: 10.1186/1479-5876-4-10.
9. Mitchell J A., Gillam E M., Stanley L A., et al Immunotoxic side-effects of drug therapy. Drug Saf. 1990 May-Jun;5(3):168-78. doi: 10.2165/00002018-199005030-00002.
10. Sim E. Drug-induced immune-complex disease. Complement Inflamm. 1989;6(2):119-26. doi: 10.1159/000463084.
11. Hofstra A H., Uetrecht J P. Reactive intermediates in the oxidation of hydralazine by HOCl: the major oxidant generated by neutrophils. Chem Biol Interact. 1993 Dec;89(2-3):183-96. doi: 10.1016/0009-2797(93)90008-m.
12. Yu B., Han Y., Zhang J. et al. Acute Tumor Infammation with CD4/8+ and CD11+ Prolong the Survival Effect Induced by Intratumral Injection Optimum Combination of Chemotherapy Drugs with Hydralazine as Hapten in Animal Model. Japanese Journal of Gastroenterology and Hepatology. (2022), May, V8 (17): 1-7
13. Ding Z., Wang N., Ji N., et al. Proteomics technologies for cancer liquid biopsies. Mol Cancer. 2022 Feb 15;21(1):53. doi: 10.1186/s12943-022-01526-8.
14. Bao XH., Chen BF., Liu J., et al. Olink proteomics profiling platform reveals non-invasive inflammatory related protein biomarkers in autism spectrum disorder. Front Mol Neurosci. 2023 May 24:16:1185021. doi: 10.3389/fnmol.2023.1185021. eCollection 2023.
15. Wang X., Nissen M., Gracias D., et al. Single-cell profiling reveals a memory B cell-like subtype of follicular lymphoma with increased transformation risk. Nat Commun. 2022 Nov 9;13(1):6772. doi: 10.1038/s41467-022-34408-0.
16. Qiu, X.J., Hill, A., Packer, J., et al. Single-cell mRNA quantification and differential analysis with Census. Nat Method. 2017 Mar; 14(3):309-315. doi: 10.1038/nmeth.4150. Epub 2017 Jan 23.
17. Andreatta, M., Carmona, S.J. UCell: Robust and scalable single-cell gene signature scoring. Comput Struct Biotechnol J. 19,3796-3798 (2021).
18. Ebright RY., Lee S., Wittner BS., et al. Deregulation of ribosomal protein expression and translation promotes breast cancer metastasis. Science. 2020 Mar 27;367(6485):1468-1473. doi: 10.1126/science. aay0939. Epub 2020 Feb 6.
19. Schneider WM., Chevillotte MD., Rice CM. Interferon-stimulated genes: a complex web of host defenses. Annu Rev Immunol. 2014:32:513-45. doi: 10.1146/annurev-immunol-032713-120231. Epub 2014 Feb 6.
20. Lin M., Zhang Z., Gao M., et al. MicroRNA-193a-3p suppresses the colorectal cancer cell proliferation and progression through downregulating the PLAU expression.Cancer Manag Res. 2019 Jun 12:11:5353-5363. doi: 10.2147/CMAR.S208233. eCollection 2019.
21. Mitri DD., Toso A., Chen JJ., et al. Tumour-infiltrating Gr-1+ myeloid cells antagonize senescence in cancer. Nature. 2014 Nov 6;515(7525):134-7. doi: 10.1038/nature13638. Epub 2014 Aug 24.
22. Havel JJ., Chowell D., Chan TA. The evolving landscape of biomarkers for checkpoint inhibitor immunotherapy. Nat Rev Cancer. 2019 Mar;19(3):133-150. doi: 10.1038/s41568-019-0116-x.
23. Yao RQ., Zhao PY., Li ZX., et al. Single-cell transcriptome profiling of sepsis identifies HLA-DRlowS100Ahigh monocytes with immunosuppressive function. Mil Med Res. 2023 Jun 19;10(1):27. doi: 10.1186/s40779-023-00462-y.
24. Asano N., Matsuzaki J.,Ichikawa M., et al. A serum microRNA classifier for the diagnosis of sarcomas of various histological subtypes. Nat Commun. 2019 Mar 21;10(1):1299. doi: 10.1038/s41467-019-09143-8.
25. Terekhova M., Swain A., Bohacova P., et al. Single-cell atlas of healthy human blood unveils age-related loss of NKG2C+GZMB-CD8+ memory T cells and accumulation of type 2 memory T cells. Immunity. 2023 Dec 12;56(12):2836-2854.e9. doi: 10.1016/j.immuni.2023.10.013. Epub 2023 Nov 13.
26. Lutz V., Hellmund VM., Picard FSR., et al. IL18 Receptor Signaling Regulates Tumor-Reactive CD8+ T-cell Exhaustion via Activation of the IL2/STAT5/mTOR Pathway in a Pancreatic Cancer Model. Cancer Immunol Res. 2023 Apr 3;11(4):421-434. doi: 10.1158/2326-6066.CIR-22-0398.
27. Vecchié A., Bonaventura A., Toldo S., et al. IL-18 and infections: Is there a role for targeted therapies? J Cell Physiol. 2021 Mar;236(3):1638-1657. doi: 10.1002/jcp.30008. Epub 2020 Aug 13.
28. Zhang YJ., Zhong XP., Chen Y., et al. Association between CASP-8 gene polymorphisms and cancer risk

in some Asian population based on a HuGE review and meta-analysis. Genet Mol Res. 2013 Feb 28;12(4):6466-76. doi: 10.4238/2013. February.28.3.
29. Zhou S., Lu H., Xiong M. Identifying Immune Cell Infiltration and Effective Diagnostic Biomarkers in Rheumatoid Arthritis by Bioinformatics Analysis. Front Immunol. 2021 Aug 13:12:726747. doi: 10.3389/fimmu.2021.726747. eCollection 2021.
30. Chiang SK., Chen SE., Ling-Chu Chang LC. The Role of HO-1 and Its Crosstalk with Oxidative Stress in Cancer Cell Survival. Cells. 2021 Sep 13;10(9):2401. doi: 10.3390/cells10092401.
31. Guo Y., Chen T., Liang X., et al. Tumor Cell Derived Exosomal GOT1 Suppresses Tumor Cell Ferroptosis to Accelerate Pancreatic Cancer Progression by Activating Nrf2/HO-1 Axis via Upregulating CCR2 Expression. Cells. 2022 Dec 2;11(23):3893. doi: 10.3390/cells11233893.
32. Li J., Byrne KT., Yan F., et al. Tumor Cell-Intrinsic Factors Underlie Heterogeneity of Immune Cell Infiltration and Response to Immunotherapy. Immunity. 2018 Jul 17;49(1):178-193.e7. doi: 10.1016/j.immuni.2018.06.006. Epub 2018 Jun 26.
33. Bluestein BM., Morrish F., Graham DJ., et al. Analysis of the Myc-induced pancreatic β cell islet tumor microenvironment using imaging ToF-SIMS. Biointerphases. 2018 Aug 28;13(6):06D402. doi: 10.1116/1.5038574.
34. Peng J., Sun BF., Chen CY., et al. Single-cell RNA-seq highlights intra-tumoral heterogeneity and malignant progression in pancreatic ductal adenocarcinoma. Cell Res. 2019 Sep;29(9):725-738. doi: 10.1038/s41422-019-0195-y. Epub 2019 Jul 4.

